論文 Analyses of Concrete Columns Confined with Lateral Reinforcements

Ha-Won SONG[*1], Dong-Hue CHOI[*2], Keun-Joo BYUN[*3] and Koichi MAEKAWA[*4]

ABSTRACT: In this paper, experiments and analyses for concrete columns confined with lateral reinforcements are conducted to investigate the confining effect of confined concrete columns having different core sizes, spacing ratios and lateral reinforcement ratios. Results of the analyses obtained using the continuum fracture and plasticity model for the prepeak behavior of confined concrete columns and simple strain-localization model for the post-peak behavior of the columns are analyzed and compared with experimental results.
KEYWORDS: lateral reinforcements, experiments, confined concrete columns, continuum fracture and plasticity, strain-localization model.

1. INTRODUCTION

The concrete columns properly confined with lateral reinforcements gain increased strength and ductility. The confining effect of confined concrete columns has close relation to lateral displacements of concrete core under compression. For evaluating of the confining effect, the confinement effectiveness index defined as the ratio of confining stress to maximum confining stress in confined concrete columns were used usefully[1]. In this paper, the prediction models of prepeak and post-peak behaviors of confined concrete columns are discussed, which can be used usefully for confining reinforcement design.

2. EXPERIMENTS FOR CONFINED CONCRETE COLUMNS

To evaluate behaviors of confined concrete columns, experiments are done for rectangular confined concrete columns with lateral reinforcements as shown in **Fig.1**. Because the confining effect occurs after failure of concrete cover, the concrete cover is neglected. Round rebars (yield strength : 3000kgf/cm^2, reinforcement diameter : ϕ6, ϕ9, ϕ12, ϕ16) are also used to eliminate bond effect. In order to get ideal confining effect only by lateral reinforcement, joint of lateral reinforcement is welded and longitudinal reinforcements are neglected in the experiment. Details of the specimen set a, b, c and d are summarized in **Table 1**. Study parameters of specimens are also remarked in **Table 1**. The prepeak and post-peak mean axial stress-strain relationships of the specimens were

*1 Department of Civil Eng., Yonsei Univ., Seoul, Korea, Ph.D., Member of JCI
*2 Department of Civil Eng., Yonsei Univ., Seoul, Korea, ME
*3 Department of Civil Eng., Yonsei Univ., Seoul, Korea, DR, Member of JCI
*4 Department of Civil Eng., Univ. of Tokyo, Tokyo, Japan, DR, Member of JCI

obtained by measuring overall logitudinal displacement of column under fixed end surfaces conditions by LVDTs and the strain of lateral reinforcements were measured by two pairs of steel strain gauges at lateral tie located at the center of each column. As shown at **Fig.2**, the unconfined concrete columns show brittle failure mode, but confined concrete columns show failure mode by a shear band. The experimental results will be shown with analysis results later in this paper.

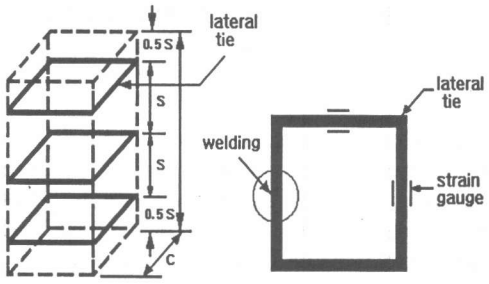

Fig.1 Detail of lateral reinforcement

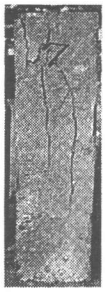

(a)Unconfined concrete column

(b)Confined concrete column

Fig.2 Failure modes of concrete columns

Table.1 Details of column specimens

Set	Specimen No. (#)	Specimen Size (cm)	Core Size (c) (cm)	Tie Spacing (s) (cm)	Spacing Ratio (s/c)	Volumetric Reinforcement Ratio (ρ_v)(%)	Lateral Reinforcement	Remark	
a	1	15×15×60	14.1	7	0.53	2.58	ϕ 9	Size Effect of Core	
	2	20×20×80	18.7	9.5	0.51	2.55	ϕ 12		
b	3	20×20×80	19.4	3.2	0.16	1.82	ϕ 6	ρ_v = 1.9%	Effect of Spacing
	4	20×20×80	19.1	7	0.37	1.90	ϕ 9		
	5	20×20×80	18.7	13	0.70	1.86	ϕ 12		
	6	20×20×80	18.4	23	1.25	1.90	ϕ 16		
c	7	20×20×80	19.1	3.8	0.20	3.51	ϕ 9	ρ_v = 3.5%	
	8	20×20×80	18.7	7	0.37	3.46	ϕ 12		
	9	20×20×80	18.4	12.3	0.67	3.55	ϕ 16		
d	10	18×18×54	17.1	6	0.35	2.48	ϕ 9	Size Effect of Length	
	11	18×18×72	17.1	6	0.35	2.48	ϕ 9		
	12	20×20×80	-	-	-	Plain Concrete			

3. ANALYSIS MODELS OF CONFINED CONCRETE COLUMNS

The constitutive models of confined concrete columns consist of continuum fracture and plasticity model for prepeak behaviors as shown at **Fig.3(a)** and strain-localization model for post-peak behaviors as shown at **Fig.3(b)**. The concrete in the constitutive model for the prepeak behavior is regarded as a damaged continuity having elasto-plasticity and the model is implemented into 3D FEM program[2]. Then FEM analyses based on concrete idealized as solid elements and steel as beam elements are carried out for one-fourth portion of column. The post-peak behavior of concrete is characterized by shear band formation at the localized zone and elastic unloading in non-localized zone.

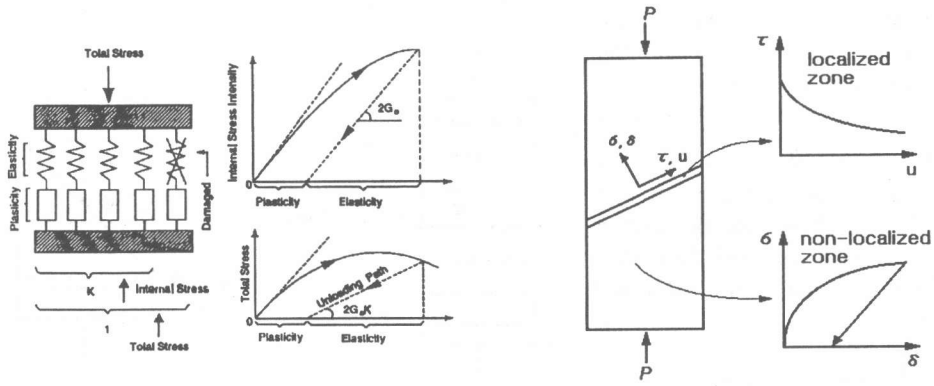

(a) prepeak model **(b) post-peak model**

Fig.3 Schematic outline of prepeak and post-peak models

3.1 CONTINUUM FRACTURE AND PLASTICITY MODEL

The nonlinear behavior of concrete is indicated by the plasticity, which denotes the residual deformation, and the internal damage, which represents the loss of the elastic shear stiffness induced by the occurrence of micro-defects and the internal stress intensity. Micro-defects were found not to affect the volumetric elastic energy capacity of concrete but the elastic energy capacity in shear mode. Maekawa et al. introduced the fracture parameter K to indicate the fracturing damage occuring in shear elasticity of concrete, and proposed the second invariant of elastic shear strains J_{2e} as the primary indicator of internal stress intensity which evolves the continuum damage associated with the assembly of micro-defects. The damaging is formulated being suppressed by the 3-dimensional confinement denoted by I_{1e} as well. The plastic indicator J_{2p} is considered to represent the induced permanent deformation in shear mode and the isotropic plastic indicator I_{1p} is formulated as the inelastic dilatancy. The value of K and J_{2e} are related to the strength gain of confined columns and J_{2p} to the ductility. The details of the constitutive laws and FEM modeling are discussed in references[1,2].

3.2 STRAIN-LOCALIZATION MODEL

The post-peak behaviors of confined concrete columns, loaded in compressive stress σ, can be modeled by the formation of shear band having uniform angle restrained by lateral reinforcement and the cohesion of concrete as shown at **Fig.4**. The post-peak behaviors are characterized and modeled as the localized behaviors in the shear failure plane localized by increasing microcrack and the elastic unloading in the non-localized zone. For the purpose of analyzing post-peak behaviors of confined concrete columns, strain-localization behaviors of concrete columns with lateral reinforcement is modeled by localized zone which is characterized by shear band and non-localized zone which is characterized by separated two concrete cores.

In the localized zone, the sliding of shear band occurs due to the cohesion of concrete or aggregate interlocking. **Fig.5** shows strain-localization model acting on shear failure plane having failure angle θ by compressive stress σ_{cc} and horizontal effective confining stress σ_h which can be obtained from confining effect of lateral reinforcements.

The shear stress τ and vertical stress σ at shear failure plane can be written as Eq. 1a, 1b.

$$\tau = (\sigma_h - \sigma_{cc}) \sin\theta \cos\theta \quad (1a)$$

$$\sigma = -\sigma_h \cos^2\theta - \sigma_{cc} \sin^2\theta \quad (1b)$$

The yield function f at shear failure plane can be written as Eq. 2 with internal hardening coefficient α and stress deviator tensors s_{ij},

$$f = \sqrt{\frac{3}{2} s_{ij} : s_{ij}} + \alpha \left(\frac{1}{3} \sigma_{ii} - p_o \right) \quad (2)$$

where, $\alpha = \dfrac{6 \sin\phi}{3 - \sin\phi}$, $p_o = \dfrac{\tau_{o,\max}}{\tan\phi}$ and ϕ is the friction angle of concrete. The cohesion of concrete at maximun stress $\tau_{o,\max}$ can be written as follows,

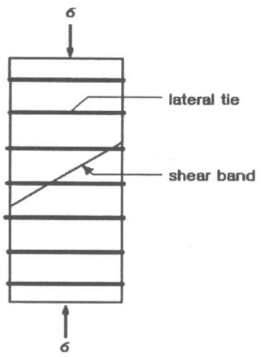

Fig.4 Formation of shear band

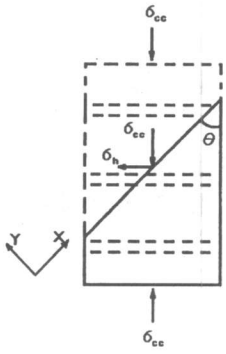

Fig.5 Model of strain-localization

$$\tau_{o,\max} = [\sigma_{cc}(\cos\theta - \sin\theta) - \sigma_h(\sin\theta + \cos\theta)] \cdot \sin\theta \quad (3)$$

By substituting Eq. 1 into Eq. 2, i.e., $f = 0$, the compressive stress of confined concrete σ_{cc}, which is function of the shear band angle θ, is obtained as follows,

$$\sigma_{cc}(\theta) = \frac{\sigma_h (\sqrt{3} \sin\theta + \alpha \cos\theta) \cos\theta + \alpha P_o}{(\sqrt{3} \cos\theta - \alpha \sin\theta) \sin\theta} \quad (4)$$

Then, the compressive stress at shear failure plane of concrete after the peak can be expressed with θ which is obtained by equating $\sigma_{cc}(\theta)$ and peak strength.

$$\sigma_{cc}(u) = \frac{\tau_o(u)}{\sin\theta(\cos\theta - \sin\theta \tan\phi)} + \sigma_h \tan(\phi + \theta) \quad (5)$$

where, $\tau_o(u)$ is relationship curve between the cohesion of concrete and the sliding u obtained from experiments as shown at **Fig.6**. Then, the strain after the peak can be obtained as Eq. 6 below by considering the strain occurred up to the peak ε_{cc}, the strain occurred by the sliding in the shear failure plane and the strain decreased by elastic recovery in the non-localized zone, respectively, i.e.

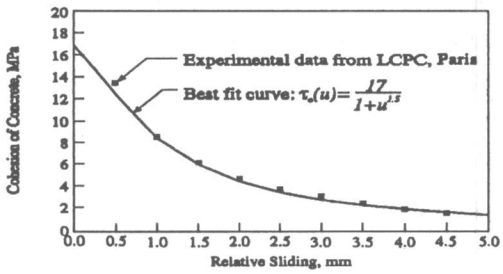

Fig.6 Evolution of cohesion of concrete at shear failure plane[3]

$$\varepsilon(u) = \varepsilon_{cc} + \frac{u \cos\theta}{L} - \frac{1}{E_c}(\sigma_{cc}(\theta) - \sigma_{cc}(u)) \quad (6)$$

where, L is length of column and E_c is concrete elastic modulus.

4. COMPARISON OF RESULTS BY ANALYSES AND EXPERIMENTS.

Table 2 shows results of analyses and experiments. For specimen set a having different core sizes of 14.1, 18.7cm, it can be seen that the size of the core has no significant influence on the confinement of columns. The results of set d also shows that the specimen lengths have no significant influence on the behaviors of concrete columns.

Table.2 Results of experiments and analyses

Specimen No.		Core Peak Strength σ_{cc} (kg/cm^2)		Strain at Peak Strength ε_{cc}		Strength Gain (kg/cm^2)		Confining Stress of Concrete at Peak σ_v (kg/cm^2)		Confinement Effectiveness Index α_{eff}	
		Analysis	Exp.	Analysis	Exp.	Analysis	Exp.	Analysis	Exp.	Analysis	Exp.
set a	1	337.0	348.5	0.00510	0.0051	94.0	105.5	13.43	9.68	0.35	0.25
	2	334.8	352.8	0.00510	0.0045	91.8	109.8	12.94	9.57	0.34	0.25
set b	3	322.3	332.5	0.00479	0.0050	79.3	89.5	9.54	9.24	0.35	0.34
	4	306.9	335.7	0.00469	0.0046	63.9	92.7	10.51	11.30	0.37	0.40
	5	287.6	332.0	0.00465	0.0042	44.6	89.0	8.21	9.28	0.29	0.33
	6	268.1	326.7	0.00419	0.0038	25.1	83.7	2.85	3.73	0.10	0.13
set c	7	355.7	340.5	0.00533	0.0043	112.7	97.5	19.79	14.10	0.38	0.27
	8	333.1	386.8	0.00517	0.0050	90.1	143.8	18.56	23.18	0.36	0.45
	9	298.0	314.3	0.00531	0.0042	55.0	71.3	13.22	12.96	0.25	0.24
set d	10	351.0	361.2	0.00511	0.0059	108.0	118.2	14.33	15.88	0.32	0.24
	11	350.2	341.5	0.00510	0.0042	107.2	98.5	14.32	12.65	0.32	0.20

The effective confining stress σ_v is the volumetric average of the lateral confining stress induced in the concrete at peak strength and confinement effectiveness index α_{eff} is defined as σ_v normalized by maximum confinement $\sigma_{v,\lim}(=-(1/2)\rho_v f_y)$. **Fig.7** and **Fig.8** show analyses and experimental results of set b(ρ_v=1.9%) and set c(ρ_v=3.5%) respectively for the cases of different spacing ratios (s/c). The reduction of the spacing ratios results in increases of the peak strength, strain at peak strength and effective confining stress.

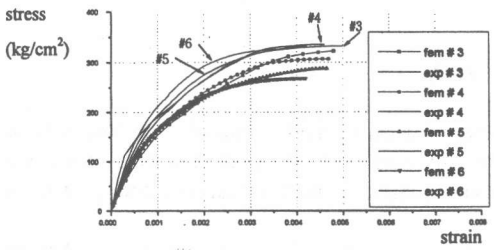

Fig.7 Results for different spacing ratios (ρ_v=1.9%)

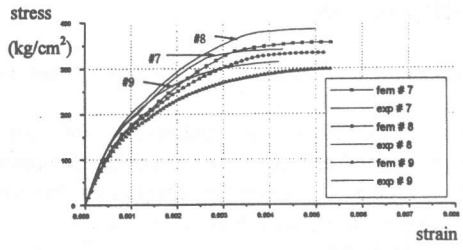

Fig.8 Results for different spacing ratios (ρ_v=3.5%)

Fig.9～12 show that post-peak stress and strain curve with shear band failure is well simulated by strain-localization model.

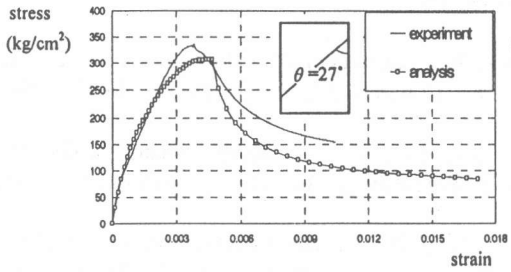

Fig.9 Result of model #4

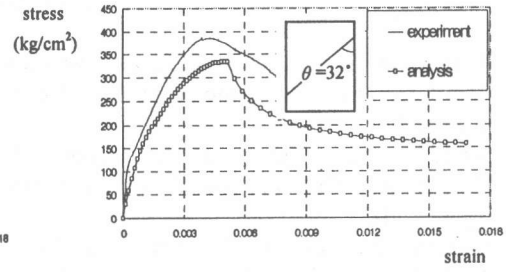

Fig.10 Result of model #8

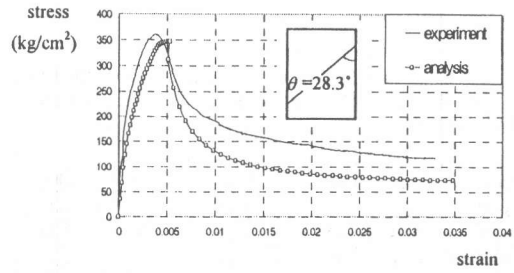

Fig.11 Result of model #10

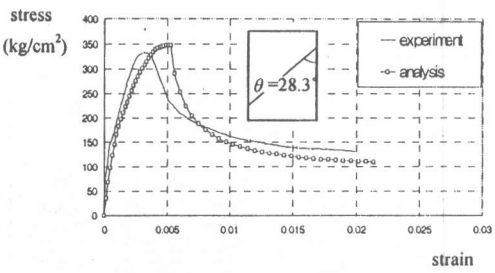

Fig.12 Result of model #11

Fig.13 shows the relationship between spacing ratios (s/c) and effective confining stress σ_v from experiments and analyses for ρ_v=1.9% and ρ_v=3.5%. The reduction of the spacing ratios results in increases of the effective confining stress. But the columns having spacing ratio of 0.2 results in an decrease of effective confining stress due to eccentric failure in experiment for ρ_v=3.5% and due to use of small diameter (ϕ6) of lateral reinforcements for ρ_v=1.9%.

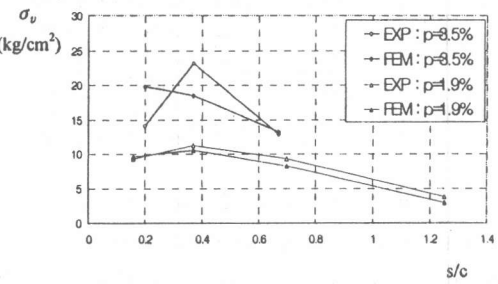

Fig.13 Relationship between spacing ratio and effective confining stress

5. CONCLUSION

The following conclusions are obtained from this study.

(1) For evaluating the behaviors of concrete columns with lateral reinforcements, experiments are done with confined concrete columns and analyses are also done for the prepeak behavior by continuum fracture and plasticity model and for the post-peak behavior by strain-localization model.
(2) The 3D FEM analysis is confirmed to be used for the analysis of the prepeak behavior of confined concrete columns effectively and strain-localization model also predicts comparably the softening behaviors for the post-peak behaviors.
(3) Decreased confining effect due to the increase of spacing ratios under constant volumetric reinforcements is confirmed from the experiment and the analyses.

REFERENCES

1. Pallewatta, T. M., Irawan, P. and Maekawa, K., "Confinement Effectiveness of Lateral Reinforcement Arrangements in Core Concrete", Concrete Library of JSCE, No.27, 1996, pp.197-223.
2. Maekawa, K., Takemura, J., Irawan, P. and Irie, M., "Triaxial Elasto-Plastic and Continuum Fracture Model for Concrete", Proceedings of JSCE, 460/V-18, 1993, pp.131-138.
3. Cusson, D., Larrard, F., Boulay, C. and Paultre, P., "Strain Localization in Confined High-Strength Concrete Columns", ASCE Structural Engineering, Vol.122, No.9, 1996, pp.1055-1061.